SPATIO-TEMPORAL ANALYSIS OF TURBIDITY IN THE PRAYAGRAJ REGION, UTTAR PRADESH USING NDTI FROM SENTINEL-2 IMAGERY

Submitted by HARIPRIYA K R (Register Number: 243308)

In partial fulfilment of the requirements for the award of

Master of Science in Data Analytics and Geoinformatics

for

Geospatial Programming

School of Digital Sciences Kerala University of Digital Sciences, Innovation and Technology

(Digital University Kerala)

Technocity Campus, Thiruvananthapuram, Kerala – 695317

JUNE 2025

BONAFIDE CERTIFICATE

This is to certify that the project report entitled

"SPATIO-TEMPORAL ANALYSIS OF TURBIDITY IN THE PRAYAGRAJ REGION, UTTAR PRADESH USING NDTI FROM SENTINEL-2 IMAGERY"

submitted by **HARIPRIYA K R** (Reg. No: 243308)

in partial fulfilment of the requirements for the award of the degree of

Master of Science in Data Analytics and Geoinformatics

in the domain of **Geospatial Programming**, is a bona fide record of the work carried out by her under our supervision at **Kerala University of Digital Sciences, Innovation and Technology**

Supervisor

Dr. Radhakrishnan T

Assistant professor

DUK

ORGANISATIOJN CERTIFICATE BLANK PAGE FOR PAGE NUMBER

DECLARATION

I, HARIPRIYA K R, a student of Data Analytic and Geoinformatics, hereby declare that this report is substantially the result of my own work, except, where explicitly indicated in the text and has been carried out dur- ing the period February 2025 – June 2025.

Place: DUK

Date: June HARIPRIYA K R

ACKNOWLEDGEMENT

I hereby express my sincere and profound gratitude to my supervisors,

Dr. Radhakrishnan, Assistant Professor, Digital University Kerala, and **Mrs. Anju S.**, Software Engineer at the Centre for Geospatial Analytics, Digital University Kerala, for their invaluable guidance, insightful suggestions, and constant encouragement throughout the course of this project. Their support played a crucial role in shaping the direction and outcome of this work.

I am also thankful to the esteemed faculty members and dedicated staff of **Kerala University of Digital Sciences, Innovation and Technology** for providing a supportive academic environment and access to the necessary infrastructure and resources. Their contributions were essential to the successful completion of this research.

I extend my sincere appreciation to my peers and classmates for their helpful discussions, collaboration, and continued motivation, which enriched both the academic and practical aspects of this journey.

Finally, I would like to thank my family for their unwavering support, patience, and encouragement throughout the project. Their belief in me has been a constant source of strength and inspiration.

The successful completion of this project would not have been possible without the collective support of all the above individuals. I am deeply grateful to each one of them.

HARIPRIYA K R
Register Number: 243308

ABSTRACT

This study investigates seasonal turbidity variation in the Prayagraj region of Uttar Pradesh from 2019 to 2024 using the Normalized Difference Turbidity Index (NDTI) derived from Sentinel-2 Surface Reflectance (SR) satellite imagery. The Area of Interest (AOI) is a 15 km buffer around the city centre, covering parts of the Ganga, Yamuna, and their confluence at the Triveni Sangam—a site globally recognized for hosting the largest human river-bathing gatherings, including the Kumbh Mela and Magh Mela.Monthly median composites for pre-monsoon (May) and post-monsoon (October) were analysed. Water bodies were identified using the Normalized Difference Water Index (NDWI), and NDTI was computed to assess relative turbidity. Temporal trends were evaluated using Z-scores and linear regression, while spatial turbidity shifts were captured through year-on-year difference composites (ΔNDTI). Findings reveal a gradual increase in turbidity during pre-monsoon months, likely due to recurring mass gatherings and reduced river flow. Post monsoon turbidity was more variable and primarily shaped by monsoon runoff and sedimentation. High NDTI values consistently aligned with active ghats (stepped structures along the riverbank used for ritual bathing and public access to water). This study demonstrates the effectiveness of NDTI-based geospatial monitoring in understanding the combined impacts of seasonal hydrology and human activity in culturally and environmentally dynamic riverine systems

TABLE OF CONTENTS

LIST OF FIGURES

LIST OF SYMBOLS

Symbol	*Definition*
NDTI	*Normalized Difference Turbidity Index*
NDWI	*Normalized Difference Water Index*
∆NDTI	*Year-on-year change in NDTI*
Z	*Z-score (standardized value)*
μ	*Mean of NDTI values*
σ	*Standard deviation of NDTI values*
R²	*Coefficient of determination (goodness-of-fit of regression line)*
x	*Observed value*
y	*Predicted value (in trend line)*
m	*Slope of the linear trend line*
c	*Intercept of the linear trend line*

1. INTRODUCTION

1.1 Background

Rivers play a vital role in sustaining ecosystems, cultural practices, and urban life. In India, rivers like the Ganga and Yamuna are not only ecological lifelines but also central to gatherings and social events. However, their water quality is frequently affected by both natural and anthropogenic factors, particularly turbidity, which indicates the presence of suspended particles such as silt, clay, and organic matter. Monitoring turbidity is essential for understanding river health, especially in regions with seasonal crowd gatherings, monsoon runoff, and urban discharge. Traditional in-situ turbidity measurement is often limited in spatial and temporal coverage. To overcome this, satellite-based indices like the Normalized Difference Turbidity Index (NDTI) have emerged as effective tools for largescale, consistent, and time-efficient turbidity assessment. This study uses multi-year Sentinel-2 imagery to monitor turbidity changes across seasons, with a focus on the Prayagraj region, where crowd-driven and natural influences intersect.

1.2 Remote-Sensing Indices & NDTI

Remote sensing indices are mathematical expressions applied to satellite image bands to extract specific surface information. In water quality monitoring, spectral indices like the Normalized Difference Turbidity Index (NDTI) help quantify turbidity levels in river systems. These indices simplify complex reflectance data into interpretable values, making it possible to monitor water clarity, detect changes, and support environmental decision-making using satellite imagery. The following sub-sections describe the NDTI in detailed format like its formula, interpretation, and suitability for large-scale river turbidity studies.

1.2.1 Definition, Formula, Interpretation

The Normalized Difference Turbidity Index (NDTI) is a widely adopted spectral index used for estimating relative turbidity levels in surface water bodies through remote sensing. It utilizes the reflectance properties of Sentinel-2 imagery, specifically the red and green spectral bands, to detect suspended sediment concentrations.

The NDTI is computed using the following equation:

$$NDTI = Red + Green/\ Red - Green$$

Where: *Red* refers to Band 4 (B4) of Sentinel-2, which is sensitive to suspended sediments and typically exhibits higher reflectance in turbid water. *Green* corresponds to Band 3 (B3) of Sentinel-2, which is used as a contrast band due to its higher reflectance in clearer water This normalized ratio enhances the spectral difference between the red and green

reflectance, which is significantly influenced by turbidity. Turbid waters tend to exhibit higher reflectance in the red band due to increased sediment scattering, while clearer waters reflect more strongly in the green spectrum. Thus, NDTI serves as a reliable indicator for mapping spatial and temporal variations in water turbidity across large riverine or coastal environments.

In terms of interpretation, typical NDTI values range from -1 to +1. Positive values, between 0 and +1, indicate elevated turbidity levels due to higher concentrations of suspended particles. Values near zero, approximately between -0.1 and +0.1, suggest neutral or moderate turbidity conditions, while negative values, ranging from -1 to 0, generally correspond to clearer water with lower sediment content. The NDTI is valuable for both visual and statistical monitoring of turbidity patterns over time and space. Its application is particularly effective when utilizing Sentinel-2 Surface Reflectance (SR) imagery, which offers a fine spatial resolution of 10 meters and frequent revisit intervals, enabling detailed and timely assessment of turbidity dynamics in aquatic environments.

1.2.2 Advantages and Limitations of the Normalized Difference Turbidity Index

1.2.2.1 Advantages

The Normalized Difference Turbidity Index (NDTI) presents several key advantages that make it a valuable tool in remote sensing applications for water quality assessment. Firstly, it is computationally simple and widely supported by cloud-based geospatial platforms such as Google Earth Engine (GEE), which facilitates efficient large-scale processing. The index utilizes high-resolution spectral bands available from freely accessible Sentinel-2 satellite data, enabling detailed spatial analysis of turbidity patterns. Moreover, NDTI allows for dynamic and non-invasive monitoring of turbidity fluctuations over time, eliminating the need for labour-intensive and costly in-situ water sampling campaigns. This capability is particularly beneficial for ongoing environmental monitoring and management in extensive riverine and coastal systems.

1.2.2.2 Limitations

Despite its strengths, the application of NDTI is subject to certain limitations. The index is susceptible to atmospheric interference, including effects caused by varying atmospheric conditions and sun glint, which may introduce inaccuracies in reflectance measurements. Additionally, spectral reflectance from adjacent land cover types, such as vegetated or urban surfaces near water bodies, can confound turbidity signals, complicating data interpretation. A further limitation of NDTI is its provision of only relative turbidity values, rather than absolute quantitative measurements such as Nephelometric Turbidity Units (NTU). As a result, while effective for detecting trends and spatial variations, NDTI cannot directly quantify turbidity concentrations, which may require complementary field measurements or alternative remote sensing approaches.

1.3 Aim and Objectives

The aim of this study is to examine how river turbidity in the Prayagraj region varies across seasons and years, with particular attention to the influence of anthropogenic activities such as mass religious gatherings, as well as natural factors like monsoon-driven runoff and fluctuating water levels. Using the Normalized Difference Turbidity Index (NDTI) derived from multi-year Sentinel-2 imagery, the study seeks to observe where and when turbidity intensifies, and how these patterns correlate with periods of high human activity or hydrological change.

To meet this aim, the study constructs time-series NDTI composites to represent turbidity across critical months such as May and October. It also applies statistical tools including Compound NDTI Difference (ΔNDTI), NDWI-based masking, Z-score normalization, and linear trend analysis. These methods enable the identification of significant turbidity deviations and their spatial distribution. The overarching objective is to evaluate whether observable turbidity patterns correspond to anthropogenic pressures or variations in water level, thereby contributing to more informed monitoring of river health in sensitive and culturally active regions

1.4 Other Metrics and Analytical Tools

In addition to the Normalized Difference Turbidity Index (NDTI), this study employs several complementary geospatial and statistical tools to enhance the accuracy, interpretability, and seasonal comparability of turbidity assessments.

1.4.1 Compound NDTI Difference (ΔNDTI)

To analyse spatial changes in turbidity across successive years, the Compound NDTI Difference (ΔNDTI) is calculated as follows

$$\Delta NDTI\ (t+1) = NDTI\ (t+1) - NDTI(t)$$

This differencing operation generates a change detection map that highlights the variation in turbidity between two consecutive years. Positive ΔNDTI values (e.g., +0.1 to +0.6) indicate areas where turbidity has increased, reflecting zones where the water has become more turbid. Conversely, negative ΔNDTI values (e.g., –0.1 to –0.5) correspond to regions exhibiting improved water clarity and reduced turbidity.

Such spatial change maps are instrumental in identifying hotspots of erosion, sediment deposition, or anthropogenic impacts, particularly in proximity to ghats—stepped riverfront structures commonly used for bathing and ritual activities. By revealing these localized turbidity dynamics, ΔNDTI facilitates targeted environmental monitoring and management interventions

1.4.2 Normalized Difference Water Index (NDWI)

The Normalized Difference Water Index (NDWI) is employed to accurately delineate water bodies by enhancing the spectral contrast between land and water surfaces. This step is critical for creating an effective mask that excludes non-water pixels prior to the application of turbidity calculations. The NDWI is computed using the green and nearinfrared (NIR) spectral bands of Sentinel-2 imagery, according to the following formula:

$$NDWI = Green + NIR/Green - NIR$$

A threshold value of NDWI greater than zero (NDWI > 0) is applied to isolate surface water pixels. The resulting water mask ensures that turbidity indices, such as NDTI, are calculated exclusively within riverine or aquatic regions, thereby minimizing contamination from land cover, vegetation, or built infrastructure. This preprocessing step significantly improves the reliability and accuracy of turbidity assessments derived from satellite data.

1.4.3 Z-Score (Standard Score)

The Z-score is utilized to standardize the mean Normalized Difference Turbidity Index (NDTI) values for each year relative to the entire dataset, quantifying the degree to which annual turbidity deviates from the long-term average. It is calculated using the formula:

$$Z = \sigma (X - \mu)$$

where X represents the NDTI value for a given year, μ is the mean NDTI value computed across all years, and σ denotes the standard deviation of NDTI values over the entire time series. By converting raw NDTI values into standardized scores, the Z-score facilitates the identification of anomalous years exhibiting significantly higher or lower turbidity levels. This approach provides enhanced insight into outlier events that may be driven by extreme monsoon conditions, anthropogenic influences such as large-scale gatherings, or other environmental disturbances, thereby supporting more robust temporal turbidity analyses.

1.4.4 Linear Regression Analysis

A linear regression model is employed to evaluate the long-term trend in turbidity throughout the study period. This statistical approach fits a linear equation to the annual mean NDTI values, represented as:

$$y = mx + cA$$

where y is the predicted mean NDTI, x denotes the year, mmm represents the slope of the regression line (indicating the rate of change in turbidity per year), and c is the intercept. A positive slope indicates an increasing turbidity trend, implying worsening water clarity over time, whereas a negative slope suggests improving water quality.

This model provides valuable insight into whether the river system is undergoing a general improvement or degradation in turbidity. Additionally, the observed trends can be correlated with external factors such as large-scale river usage or anthropogenic activities during specific years, thereby strengthening interpretations of environmental impact over time.

positive slope implies increasing turbidity (worsening clarity), while a negative slope suggests improving water quality over time.

This statistical model helps determine whether the river is undergoing a general improvement or degradation in clarity and correlates with the presence or absence of largescale river use in that year.

1.4.5 Statistical Summary and Visualization: Mean and Standard Deviation

For each year and month under consideration, the mean and standard deviation (StdDev) of NDTI values were computed across the masked river area using the .reduceRegion() function in Google Earth Engine (GEE). The mean NDTI reflects the average turbidity level of the river system for the specified period, while the standard deviation quantifies the spatial variability in turbidity. A higher standard deviation indicates greater heterogeneity in water clarity, likely attributable to localized pollution sources or flow variations.

These statistical metrics were visualized through error-bar plots, where each year's mean turbidity is presented alongside its corresponding standard deviation range. This method offers a concise representation of both central tendency and variability, facilitating clearer comparisons between stable and volatile years, particularly during the months of May and October.

Together, these quantitative analyses constitute a comprehensive framework for understanding not only the temporal evolution of turbidity but also its spatial heterogeneity. This multi-dimensional approach enhances the study's capacity to link turbidity fluctuations to seasonal changes and large-scale human activities occurring near the Sangam in Prayagraj.

2. LITERATURE REVIEW

The literature review explores key research findings related to river turbidity monitoring using remote sensing. It provides a foundation for understanding the development, use, and limitations of the Normalized Difference Turbidity Index (NDTI) and related geospatial techniques. Emphasis is placed on how turbidity is assessed across seasons, how statistical tools support time-series analysis, and how human activities like mass gatherings affect water quality. These studies form the basis for this work's methodology and comparative analysis.

2.1 Turbidity Monitoring via Remote Sensing

Turbidity is a widely used indicator of water quality, as it reflects the presence of suspended particles like sediments, algae, and pollutants. High turbidity affects aquatic ecosystems, water treatment, and public health. Traditional monitoring methods depend on in-situ sensors and field sampling, which, although accurate, are limited by cost, scale, and temporal coverage (Alparslan et al., 2007).

With the advent of satellite remote sensing, especially the Sentinel-2 and Landsat missions, researchers have increasingly used visible spectral reflectance to estimate surface water turbidity (Nechad et al., 2010). Reflectance in the red (B4) and green (B3) bands is especially useful, as red light reflects more in turbid water, while green is more sensitive to chlorophyll and suspended matter balance. These spectral responses have led to the development of indices such as the Normalized Difference Turbidity Index (NDTI), which offers repeatable, spatially extensive turbidity estimates.

Remote sensing has also proven useful in large-scale seasonal turbidity monitoring, particularly in river systems influenced by flooding, urban discharge, or human activity. Examples include sediment tracking in the Mekong, Nile, Amazon, and Ganga river basins (Chawla et al., 2022).

2.2 Application of NDTI in Water Quality Studies

The Normalized Difference Turbidity Index (NDTI), defined as:

$$NDTI = (Red - Green) \,/\, (Red + Green)$$

has established itself as a widely adopted remote sensing metric for estimating turbidity in various aquatic environments. Its utility is particularly pronounced in optically shallow and sediment-rich water bodies, where suspended particulate matter significantly influences spectral reflectance.

Numerous studies have leveraged NDTI to monitor variations in river water clarity attributable to natural processes such as erosion and seasonal runoff, as well as anthropogenic activities. For example, research by Kundu et al. (2021) applied NDTI to characterize sediment-laden zones within the Brahmaputra and Ganga river systems, highlighting its effectiveness in large, dynamic fluvial environments.

In the Indian context, successful applications of NDTI include the monitoring of sediment distribution in the Ganga River near Varanasi, turbidity assessments of the Yamuna River in the vicinity of Delhi, and evaluations of flood-induced turbidity changes within the Mahanadi basin. Collectively, these studies underscore the reliability and practical relevance of NDTI for riverine systems experiencing substantial hydrological variability and human impact.

Nonetheless, the NDTI methodology presents certain limitations. It is susceptible to confounding influences from adjacent land cover types, including vegetation, urban infrastructure, and exposed dry sediments, which can generate false-positive turbidity signals. To mitigate this, water masks derived from indices such as the Normalized Difference Water Index (NDWI) are often employed to isolate true water pixels prior to turbidity computation. Furthermore, NDTI values represent relative turbidity measures and do not directly translate to absolute physical units such as Nephelometric Turbidity Units (NTU). Achieving high-precision turbidity quantification, therefore, necessitates calibration against in situ field measurements (Nechad et al., 2010).

2.3 Time-Series and Statistical Methods in Turbidity Analysis

The assessment of water quality dynamics over time necessitates the use of robust temporal and statistical tools. Fundamental descriptive statistics, such as the mean and standard deviation, serve as essential metrics for summarizing turbidity levels and their spatial variability. Specifically, the standard deviation provides insight into the heterogeneity of turbidity distribution, often highlighting localized variations caused by factors such as inflows from tributaries, urban drainage, or concentrated human activities near river ghats.

To enable normalized comparison of turbidity across multiple years, the Z-score (standard score) is applied. This standardization facilitates the identification of anomalous years exhibiting significantly higher or lower turbidity relative to the long-term average.

Linear regression analysis is commonly employed to detect temporal trends within NDTI time series data. A positive regression slope signifies a deterioration in water clarity through increasing turbidity, whereas a negative slope indicates an overall improvement in water quality over the monitored period. Such regression techniques have been effectively utilized in prior research, including the study by Singh et al. (2020), which analysed sediment trends in river systems during pre- and post-monsoon seasons.

Complementing these approaches, compound change analysis using the difference in successive NDTI composites (ΔNDTI) provides a spatially explicit visualization of year over-year turbidity changes. By subtracting NDTI values of consecutive years, this method identifies zones of sediment erosion, deposition, or anthropogenic influence. This spatial perspective enriches the temporal analysis by revealing not only when but also where significant turbidity shifts occur, as demonstrated in the work of Martínez et al. (2021).

2.4 Impact of Human Activities and Gatherings

Large-scale religious congregations have a profound influence on riverine water quality, particularly in densely populated regions of South Asia. In India, events such as the Kumbh Mela and Magh Mela, held at the Triveni Sangam in Prayagraj, witness the participation of millions of pilgrims engaging in bathing over brief but intense periods. These mass gatherings significantly alter the physicochemical properties of river water. Empirical studies have reported a sharp escalation in suspended particulate matter, microbial contaminants, and other water quality parameters during and shortly after such events (Singh et al., 2015; CPCB Report, 2019).

Satellite-derived indicators such as the Normalized Difference Turbidity Index (NDTI) offer a remote sensing-based framework for detecting and quantifying these changes. When aligned with time-stamped festival calendars and spatial data on ghat locations, NDTI enables the monitoring of anthropogenic turbidity fluctuations at high temporal and spatial resolutions.

Observations from various years reveal contrasting trends. In some cases, water clarity rebounds to pre-event levels shortly after the gatherings. In others, turbidity remains elevated, reflecting sustained impacts from solid waste discharge, bank destabilization, and sediment resuspension driven by intense foot traffic and infrastructural strain.

Thus, integrating crowd density data, riverbank land use mapping, and temporal turbidity indices like NDTI offers a comprehensive understanding of human–river interactions. This multidimensional approach is crucial for designing effective environmental monitoring strategies and for informing policy decisions around event planning and river conservation.

3. MATERIALS & METHODS

3.1 Study Area

This study focuses on Prayagraj, a historically and spiritually significant city in Uttar Pradesh, India, located at the confluence of the Ganga, Yamuna, and the mythological Saraswati rivers—collectively known as the Triveni Sangam. The site is renowned for hosting major religious congregations such as the Kumbh Mela and Magh Mela, which attract millions of pilgrims from across the country and abroad. These large-scale gatherings involve mass bathing rituals and extensive use of the riverbanks, exerting substantial environmental and hydrological pressure on the river system.

To ensure comprehensive spatial coverage, the Area of Interest (AOI) was defined as a circular buffer of 15 kilometres around the geographic centre of Prayagraj (latitude: 25.4358° N, longitude: 81.8463° E). This region includes major segments of the Ganga and Yamuna rivers, the confluence zone, and the riverfront areas where human activity is most concentrated. The selected AOI captures both natural variations and anthropogenic influences on river turbidity, making it well-suited for multi-temporal remote sensing analysis.

Figure 3.1-Location of Prayagraj in India

3.2 Data source

3.2.1 Satellite Imagery

The primary remote sensing dataset used in this study is the Sentinel-2 Surface Reflectance (SR) product, which was accessed through the Copernicus Open Access Hub via Google Earth Engine (GEE) and processed in Google Collab. To examine seasonal variations in river turbidity, monthly median composites were generated for two representative months in each year: May and October. May was selected to represent the pre-monsoon, dry-season period. During this time, river discharge is typically low, the channel narrows, and human activity peaks particularly due to religious events such as the Magh Mela and other local mass bathing rituals. Under these conditions, the low water volume and concentrated crowd interaction at riverbanks make the system more susceptible to turbidity disturbances. Hence, May effectively captures human-induced turbidity under minimal flow conditions. October was chosen to reflect post-monsoon dynamics, shortly after the main monsoon period of June to September. During this phase, rivers often exhibit high sediment loads resulting from upstream erosion and runoff. October is also a favourable month for satellite observations due to reduced cloud cover, wider river extents, and relatively limited human interference, making it ideal for analysing natural hydrological contributions to turbidity. The months of June to September were excluded from analysis due to persistent cloud cover and high rainfall, which compromise satellite data quality and hinder accurate turbidity estimation. Additionally, the transitional period from November to April lacks significant hydrological or anthropogenic events and was therefore not considered critical to the study's objectives. By focusing on May and October, the study ensures the capture of two distinct and contrasting turbidity conditions one dominated by human activity during the dry season and the other shaped by natural processes following the monsoon. This seasonal framing also ensures data consistency and interpretive clarity. All Sentinel2 images were cloud-masked using the Scene Classification Layer (SCL) band, and only scenes with sufficient clear-sky coverage were included in the analysis.

Figure 3.2-May month Sentinel-2 image image

Figure 3.3-October month Sentinel-2

3.2.2 Crowd/Event Data

To assess the influence of human activity on river turbidity, this study focused exclusively on riverbank locations where direct human-river interaction occurs. Specifically, five major ghats in the Prayagraj region were identified based on their frequent use for bathing, ritual immersion, and other religious activities. These locations were manually selected and geolocated using coordinate-based mapping through a Folium-based visualization interface developed during the project. The pre-monsoon season, particularly from March to May, was prioritized for crowd-based analysis, as this period coincides with heightened pilgrimage activity and large-scale religious gatherings such as the Magh Mela. During this phase, all five ghats were assumed to be actively used by the public. The selected sites include Sangam Ghat (marked in red), Arail Ghat (orange), Saraswati Ghat (blue), Daraganj Ghat (green), and Ram Ghat (purple). These colour codes were consistently applied in spatial visualizations and charts to differentiate between sites. By isolating activity at these ghats, the study aimed to correlate localized turbidity fluctuations with crowd density and seasonal human activity, thereby improving the spatial attribution of anthropogenic impact on water quality.

Figure 3.4: Folium map of highly active ghats with mass gatherings during March to May

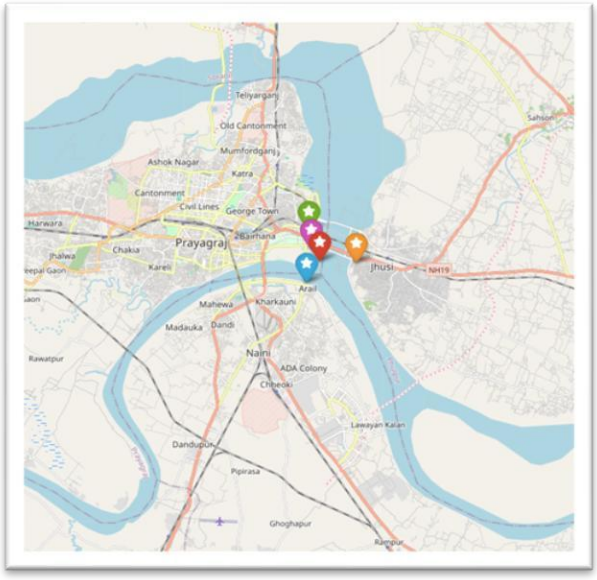

During the post-monsoon season (October), human activity along the riverbanks was significantly reduced compared to the pre-monsoon period. Based on official records and observational data, only Daraganj Ghat exhibited signs of continued public usage and mass gatherings during this time. All other ghats were inactive, with no evident river contact or large-scale events.

This seasonal variation in ghat activity was visualized through interactive Folium maps, which served as the basis for analysing spatial turbidity shifts between May and October. By focusing on periods with contrasting levels of human interaction, the study aimed to disentangle natural sediment-driven turbidity (post-monsoon) from anthropogenic influences (pre-monsoon). These observations are supported by sources such as the Prayagraj Mela Authority (2023) and the Central Pollution Control Board (CPCB, 2021).

Figure 3.5: Folium map showing active ghat with gatherings during August to September

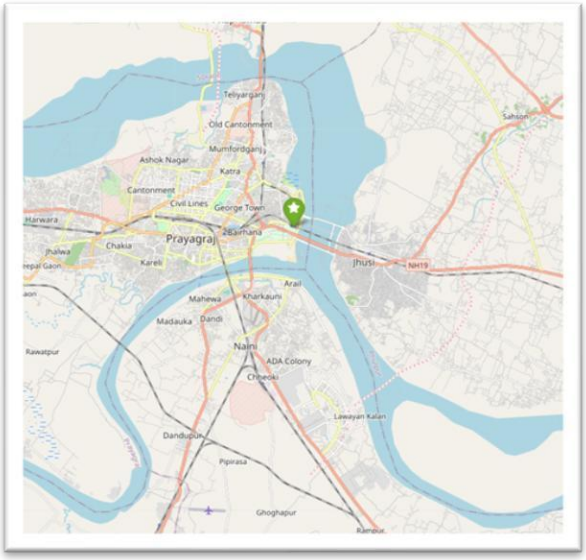

3.3 Geospatial Programming Tools

This study adopted a hybrid methodology by integrating cloud-based platforms with Python-based scripting environments to conduct the spatial and temporal analysis of river turbidity. Google Earth Engine (GEE) served as the primary platform for remote sensing data access, preprocessing, and index derivation. Sentinel-2 Surface Reflectance datasets were filtered and processed within GEE, where functions were applied to compute indices such as the Normalized Difference Turbidity Index (NDTI) and the Normalized Difference Water Index (NDWI). Cloud masking was performed using the Scene Classification Layer (SCL), and image composites were generated for the designated seasonal windows. Map layers were created to visualize RGB bands, NDTI patterns, and changes in turbidity (ΔNDTI) over time. The Earth Engine Python API (ee) and its companion library gee map were used to interface GEE operations with Python environments such as Google Colab. These tools enabled remote code execution while allowing local visualization and control over geospatial layers. Following data retrieval, statistical analysis and visual representation were performed using standard scientific Python libraries. Tabular organization and management of yearly NDTI values were handled using pandas, while numpy was used for mathematical operations such as differencing and standardization. For visual analytics, matplotlib was employed to produce time-series plots, error bar charts,

Zscore graphs, and regression lines. The scikit-learn library provided linear regression models to detect and analyse long-term trends in turbidity values. Geospatial vector processing was supported through geopandas and shapely libraries, which enabled spatial operations such as defining buffer zones and managing shapefiles. Finally, folium was used to create interactive web maps highlighting locations of key bathing ghats and crowd activity, aiding in the spatial interpretation of turbidity changes in relation to human interaction zones. This combination of GEE's large-scale satellite processing capabilities with Python's statistical and geospatial toolset facilitated a flexible, automated, and reproducible workflow for analysing the influence of natural and anthropogenic factors on water turbidity in the Prayagraj River system.

3.4 Preprocessing in Google Earth Engine (GEE)

Accurate estimation of surface water turbidity from satellite imagery requires systematic preprocessing to remove atmospheric and scene-level noise. All Sentinel-2 Surface Reflectance (SR) images used in this study were preprocessed within Google Earth Engine (GEE) to ensure the reliability of spectral indices, particularly the Normalized Difference Turbidity Index (NDTI).

One of the critical preprocessing steps involved masking out cloud and haze-affected pixels using the Scene Classification Layer (SCL) available in Sentinel-2 Level-2A products. The SCL band classifies each pixel into several land-cover and atmospheric categories. For this study, pixels corresponding to cloud shadows (class 3), medium-probability clouds (class 8), and high-probability clouds (class 9) were excluded. Only pixels labeled as clear land or water were retained for further analysis. This masking procedure significantly improved the quality of monthly composites and reduced noise in the derived NDTI values, especially for regions and months susceptible to cloud interference.

3.5 Water Masking via NDWI

To isolate water bodies and restrict turbidity calculations only to river pixels, a water mask was applied using the Normalized Difference Water Index (NDWI). NDWI was calculated from the green and near-infrared bands of Sentinel-2 imagery, with positive NDWI values typically indicating the presence of water. This mask ensured that non-water areas such as land, sandbars, and vegetation were excluded from NDTI analysis. Figure 3.6 displays the NDWI mask for the pre-monsoon period (May), illustrating river narrowing under lowflow conditions. In contrast, Figure 3.7 shows the post-monsoon NDWI mask for October, where the river appears wider due to increased upstream discharge and runoff following the monsoon season.

Figure 3.6-pre-monsoon (may) NDWI Mask

Figure 3.7-post -monsoon (October) NDWI Mask

To restrict turbidity analysis exclusively to water areas, the Normalized Difference Water Index (NDWI) was computed using Sentinel-2 spectral bands, defined as:

$$NDWI = (B3 - B8) \,/\, (B3 + B8)$$

where B3 corresponds to the green band and B8 to the Near Infrared (NIR) band. Pixels with NDWI values greater than zero were classified as water and used to generate a binary river mask based on the May 2019 median composite. This static water mask was then consistently applied across all years and months of the study period to ensure temporal comparability of turbidity assessments by excluding non-water pixels and minimizing the influence of surrounding land features.

3.6 NDTI Calculation

The Normalized Difference Turbidity Index (NDTI) was computed for each Sentinel-2 image by using the red (B4) and green (B3) spectral bands, following the formula:

$$NDTI = (B4 - B3) \,/\, (B4 + B3)$$

This index was added as a new band to each image, which then served as the basis for generating monthly median composites for the pre-monsoon (May) and post-monsoon (October) periods across the years 2019 to 2024. These composites capture seasonal turbidity variations with consistent temporal resolution.

3.7 River-Only Masking

To enhance the spatial specificity of the analysis, each NDTI composite was masked using the static river mask derived from the NDWI threshold. This masking restricts the study area to only those pixels classified as water, effectively eliminating noise from adjacent land features such as vegetation, urban infrastructure, or dry sediments. The result is a refined and precise NDTI representation of the river zone, which is crucial for accurately assessing turbidity in a complex urban environment like Prayagraj.

Figure 3.8 illustrates an NDTI map clipped exclusively to river pixels for October 2023, demonstrating the effectiveness of this masking approach.

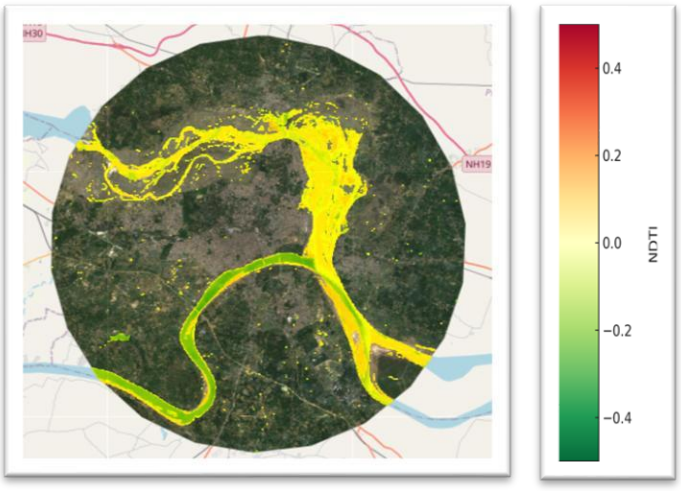

3.8 Compound NDTI Change

To examine temporal changes in turbidity, compound difference maps (ΔNDTI) were created by subtracting one year's composite from the previous year's composite for the same month. This calculation is expressed as:

$$\Delta NDTIyear\ (2) = NDTIyear\ (2) - NDTIyear\ (1)$$

For example, changes between 2020 and 2019, 2021 and 2020, and so forth were mapped. These ΔNDTI maps highlight spatial zones where turbidity has increased (positive values, depicted in red) or decreased (negative values, depicted in blue), allowing visualization of sediment buildup or erosion and other river dynamics over time.

Figure 3.9 shows an example of compound NDTI change for October 2023 compared to October 2024

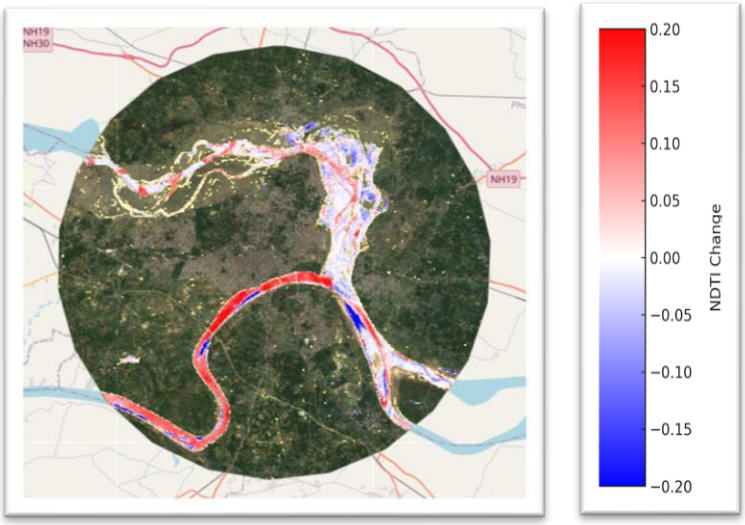

3.9 Statistical Extraction (Mean and Standard Deviation)

For each monthly NDTI composite, statistical summaries were derived to quantify spatial turbidity patterns over the study area. This was achieved using the .reduceRegion() function within Google Earth Engine (GEE), executed via its Python API in a Google Colab environment. The function was applied to the masked river area for each year and month of interest, yielding key statistical metrics including the mean and standard deviation of NDTI values. The resulting outputs were exported as Python dictionaries, which were subsequently processed and organized using the pandas library. This step produced a structured dataset for each year, allowing for consistent comparison of average turbidity levels and spatial variability across seasons and time. These statistical summaries served as the foundation for subsequent trend analysis, anomaly detection, and visualization in later sections of the study.

3.10 Time-Series Analysis in Python (Z-Score and Regression)

To assess long-term patterns in turbidity, the exported statistical summaries were analysed using Python's scientific computing stack. Z-scores were computed to standardize NDTI values and to identify years with unusually high or low turbidity relative to the multi-year mean. This standardization enabled a normalized comparison of fluctuations over time.

Additionally, linear regression models were fitted to the annual NDTI values to capture the general direction of change across the study period. This was performed using the LinearRegression module from the scikit-learn library. The models provided trendlines indicating whether turbidity increased, decreased, or remained stable over time. These analytical outputs, while derived from historical data, offered insight into the consistency of sediment behaviour in the river system and formed the basis for visual interpretations presented in later chapters**.**

4. RESULTS & COMPARATIVE ANALYSIS

4.1 Pre-Monsoon Season (May)

4.1.1 Temporal Trends in Mean NDTI and Spatial Variability (2019–2024)

Figure 4.1 illustrates the temporal variation in mean Normalized Difference Turbidity Index (NDTI) for the pre-monsoon month of May across six years (2019–2024). Each data point represents the average turbidity value calculated over the river-masked area, while the accompanying vertical error bars indicate the standard deviation, reflecting spatial variability in turbidity across the river surface.

A horizontal dashed grey line at NDTI = 0 serves as a neutral reference point. Values above this line correspond to higher turbidity (increased suspended sediment), whereas negative values indicate clearer water conditions.

The results show that 2022 and 2024 experienced elevated turbidity levels, as indicated by positive NDTI values. In contrast, the years 2019 and 2021 recorded significantly negative NDTI values, denoting comparatively clearer river water. Notably, the standard deviation peaked in 2021 and 2023, suggesting uneven spatial distribution of turbidity. Such variability is potentially influenced by localized disturbances, including sediment influx, construction near riverbanks, or human activities concentrated around urban ghats.

Figure 4.1-Mean NDTI (May) with Standard Deviation Across Years (2019–2024)

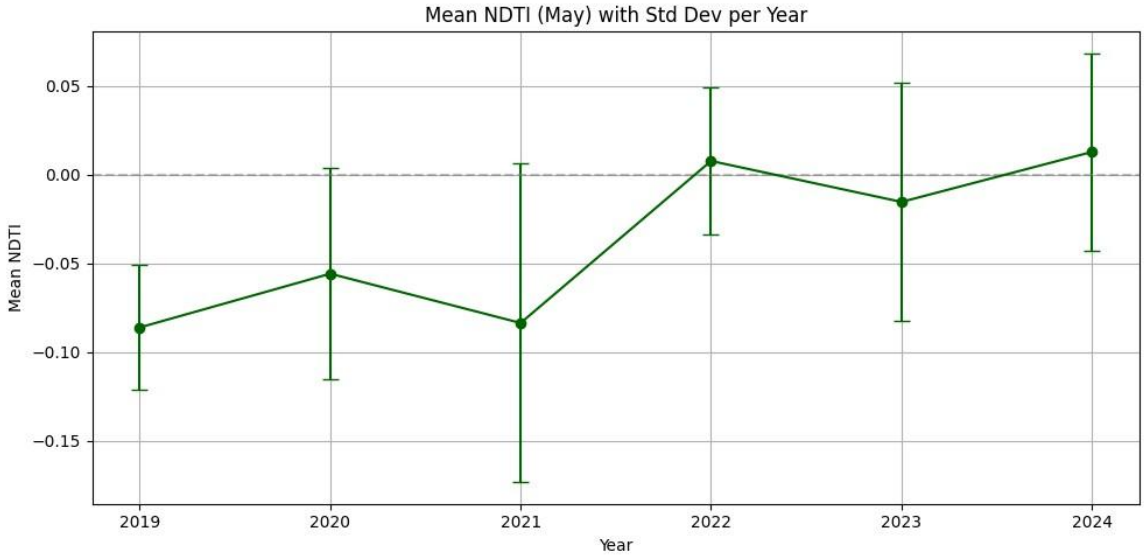

4.1.2 Z-Score Normalization of Pre-Monsoon NDTI (2019–2024)

Figure 4.2 presents the standardized Z-score values of mean NDTI for May across the study period. This transformation enables a normalized comparison of turbidity deviations relative to the dataset's overall mean. The Z-score values indicate how many standard deviations each year's mean NDTI lies above or below the six-year average.

Years with positive Z-scores experienced higher-than-average turbidity, while negative Z-scores denote clearer water conditions. Notably, 2019 and 2021 exhibited strong negative Z-scores (less than -1), highlighting periods of exceptional water clarity during the pre-monsoon season. Conversely, 2022 and 2024 recorded Z-scores exceeding +1, indicating significantly higher turbidity levels compared to the long-term mean.

These findings align with known seasonal activity patterns, where increased anthropogenic disturbance in non-Mela years especially around ghats can elevate suspended sediment levels without the benefit of large-scale river clean-up campaigns.

Figure 4.2-Z-Score of Mean NDTI (May), Standardized Across 2019–2024

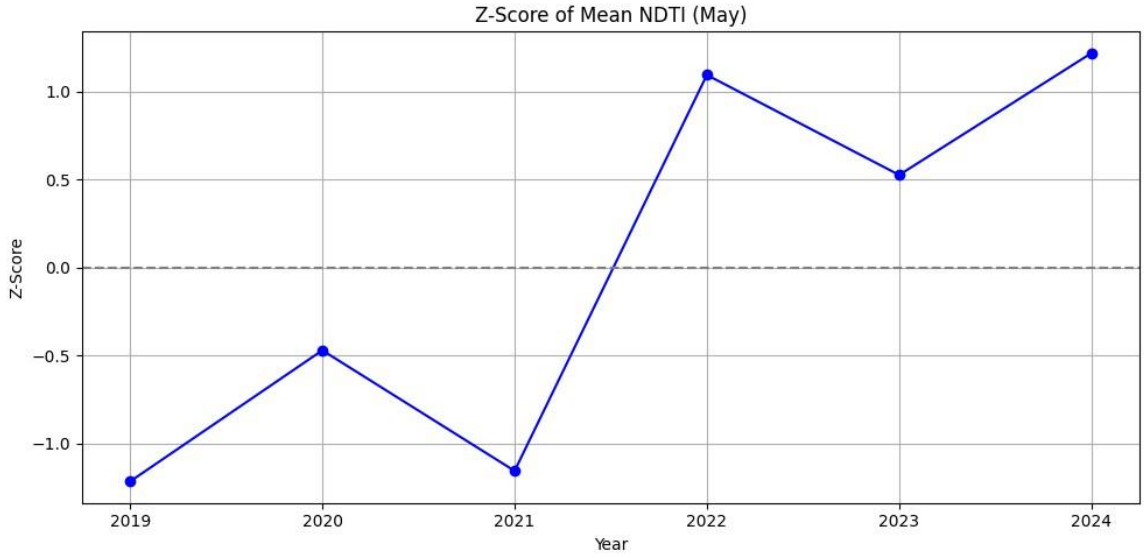

4.1.3 Linear Trend Analysis of Mean NDTI Values (May, 2019–2024)

Figure 4.3 compares the observed pre-monsoon (May) NDTI values with a linear regression model fitted to the six-year dataset. The purple line with markers represents the actual yearly mean NDTI values, while the orange dashed line denotes a regression line summarizing the historical trend over time, based on ordinary least squares fitting. A horizontal grey line at NDTI = 0 is included to indicate the neutral reference point, above which turbidity is considered elevated.

The positive slope of the regression line indicates a gradual upward trend in turbidity during the pre-monsoon period, suggesting an overall increase in suspended sediment concentration from 2019 to 2024. Although the actual annual values fluctuate, the long-term directionality reflects a steady deterioration in water clarity. This trend may be linked to cumulative anthropogenic influences such as increased waste discharge, intensifying tourism activities, and unregulated development along the riverbanks, particularly during the dry season when river flows are lower.

The analysis highlights a pattern of rising turbidity during May, with notable peaks in certain years (e.g., 2022 and 2024), pointing to a potentially growing environmental burden on the river system prior to the onset of monsoon-driven flushing.

Figure 4.3 – Linear Trend Analysis of Observed Mean NDTI Values in May (2019–2024)

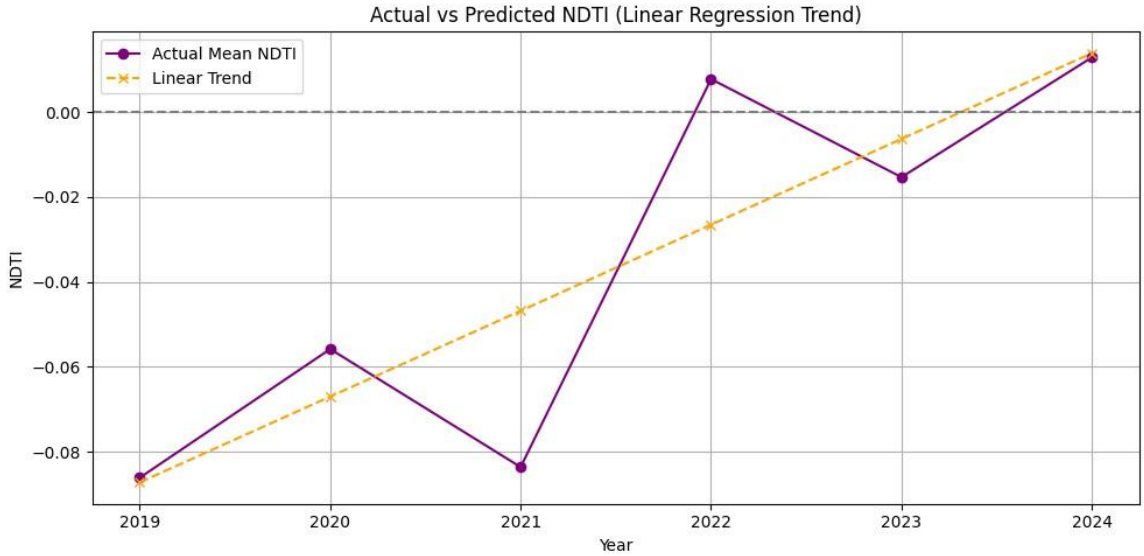

4.1.4 Spatial Distribution of Turbidity – NDTI Maps (May, 2019–2024)

Figures 4.4 to 4.9 illustrate the spatial variation in river turbidity using the Normalized Difference Turbidity Index (NDTI) across six consecutive years in the month of May. The colour gradient represents the degree of suspended sediment, ranging from green (very low turbidity) to red (high turbidity). Green areas correspond to clear water conditions, typically observed in deeper or less disturbed river sections. Yellow zones indicate low turbidity, suggesting slightly elevated sediment levels, while orange reflects moderate turbidity often associated with increased flow disturbance or localized anthropogenic activity. Red regions signify high turbidity and mark areas with intense sediment agitation, usually near major crowd or pollution hotspots.

A comparative assessment of the annual maps reveals a shift in turbidity patterns over time. From 2019 to 2021, the river consistently exhibited predominantly green and yellow zones, reflecting relatively clear water with minimal disruption. However, beginning in 2022, there is a noticeable emergence of orange zones, particularly in the vicinity of ritual entry points such as Sangam and Arail. This increase in turbidity suggests a growing influence of human-induced sediment disturbance, particularly during non-Mela periods when largescale river cleanup efforts are absent.

The spatial maps provide important contextual depth to the temporal analysis, indicating not only increasing turbidity levels over time but also highlighting specific geographic areas where sediment disturbance is becoming more concentrated and recurrent.

Figure 4.4-NDTI Map 2019, May

Figure 4.5-NDTI Map 2020, May

Figure 4.6-NDTI Map 2021, May

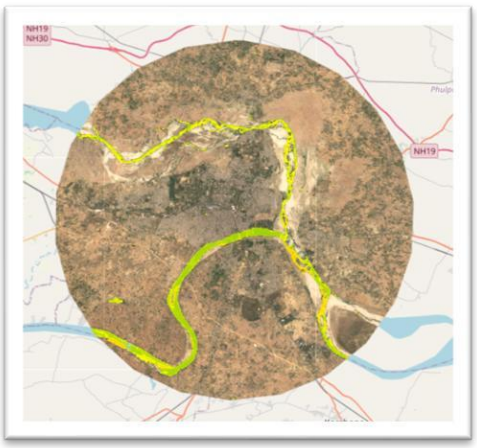

Figure 4.7-NDTI Map 2022, May

Figure 4.8-NDTI Map 2023, May

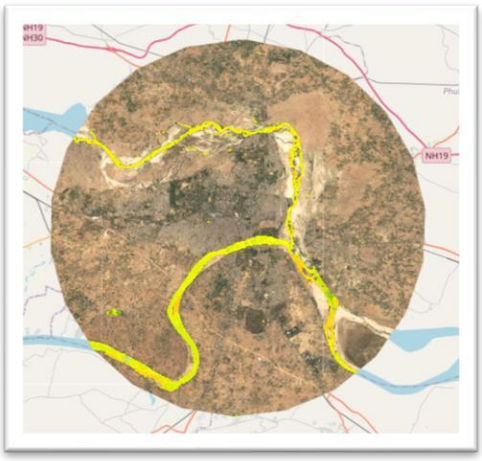

Figure 4.9-NDTI Map 2024, May

4.1.5 Year-to-Year Turbidity Variations (ΔNDTI: 2019–2024)

Figures 4.10 through 4.14 illustrate the spatial changes in turbidity levels across consecutive years during the month of May, using ΔNDTI maps. These maps represent the difference in Normalized Difference Turbidity Index (NDTI) values from one year to the next. Areas marked in red indicate an increase in turbidity compared to the previous year, while blue areas signify a decrease, reflecting clearer water conditions. White zones represent minimal or negligible change, suggesting stability in sediment levels.

Across the six-year sequence, the maps show considerable spatial variability, with some years exhibiting localized increases in turbidity and others showing reductions. Notably, red zones indicative of worsening turbidity appear more frequently and with broader spatial coverage in later years, particularly in 2022 and 2023. These regions are often aligned with known public access points along the river, where direct interaction with the water is more common during this pre-monsoon period. The timing coincides with a seasonal increase in anthropogenic activity, including bathing, tourism, and associated inflows.

While not uniform or continuous, the inter-annual shifts in turbidity suggest a cumulative influence of both natural factors (such as declining pre-monsoon flows) and human interaction. The ΔNDTI maps provide spatial evidence of where these influences may be concentrated, and they help contextualize the temporal trends observed in other sections. These findings highlight the value of combining spatial and temporal assessments when evaluating sediment dynamics in riverine systems during periods of higher surface contact and usage.

Figure 4.10-ΔNDTI (2020–2019), May

Figure 4.11-ΔNDTI (2021–2020), May

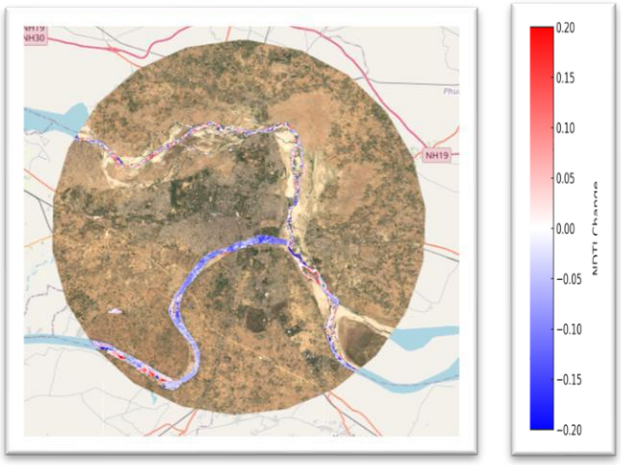

Figure 4.12-ΔNDTI (2022–2021), May

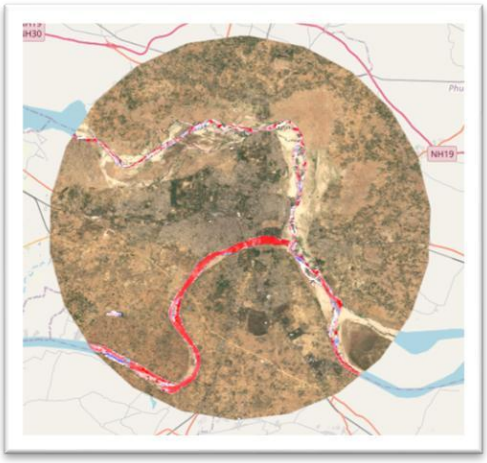

Figure 4.13-ΔNDTI (2023–2022), May

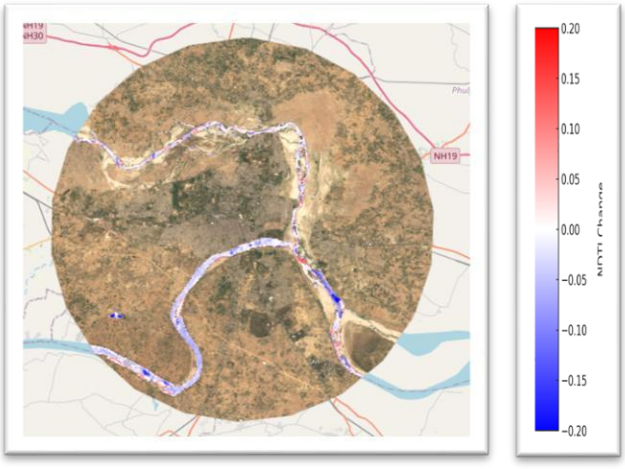

Figure 4.14-ΔNDTI (2024–2023), May

4.1.6 Compound Year-on-Year Change in NDTI with Standard Deviation (May)

Figure 4.15 presents the compound annual change in NDTI values (ΔNDTI) for the month of May, alongside the corresponding standard deviation for each year. This analysis captures the net turbidity shift from the previous year, summarizing the direction and intensity of change across the entire river segment. The data reveals that turbidity increased in 2020, 2022, and 2024, as indicated by positive ΔNDTI values, whereas 2021 and 2023 exhibited reductions in turbidity with negative ΔNDTI. Notably, the most substantial increase occurred between 2021 and 2022, where ΔNDTI peaked at approximately +0.09, suggesting a sharp rise in sediment presence during that interval.

The pattern of year-on-year change does not follow a linear progression, instead reflecting fluctuations potentially influenced by variations in crowd density, rainfall, or sediment inflow. Despite these temporal differences, the standard deviation values remain relatively consistent, ranging between 0.05 and 0.08. This stability in spatial variability suggests that although overall turbidity levels changed from year to year, the distribution of turbidity across the river surface retained a relatively uniform pattern.

Figure 4.15-Change in Compound ΔNDTI with Standard Deviation (May)

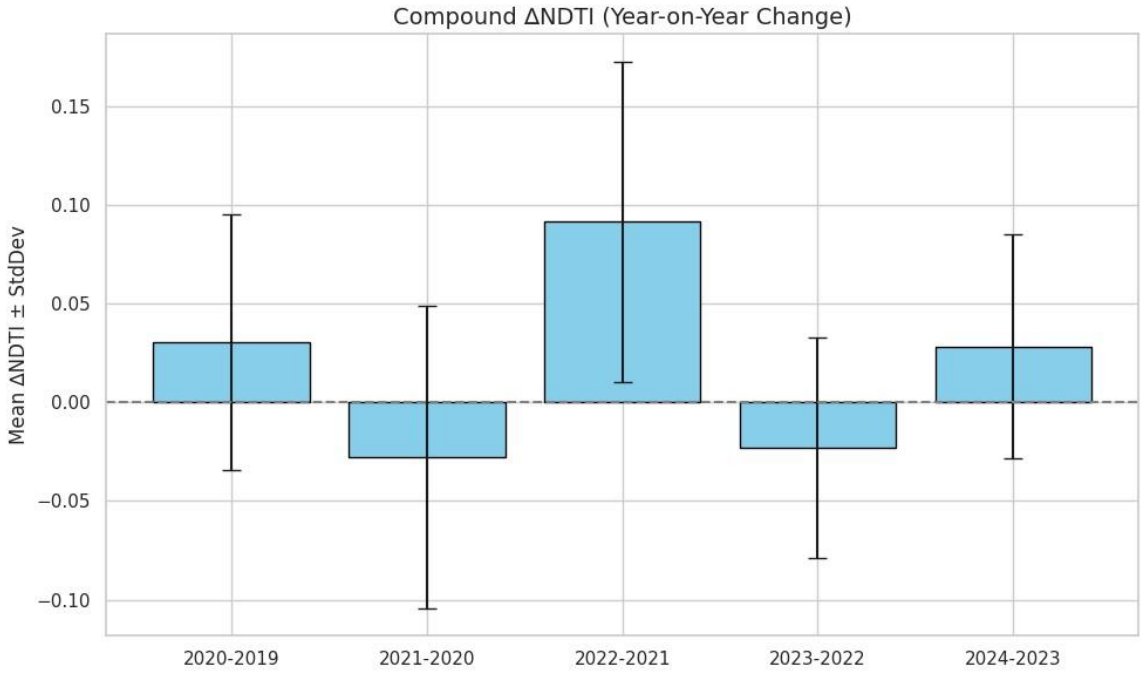

4.1 Post-Monsoon Season (October)

4.2.1 Mean NDTI and Standard Deviation (October, 2019–2024)

Figure 4.16 illustrates the post-monsoon (October) variation in average NDTI values across the study years, along with corresponding standard deviation error bars representing spatial variability in turbidity across the river surface. Each green dot marks the mean NDTI for a given year, while the grey dashed line at NDTI = 0 denotes the neutral turbidity threshold.

The data reveals notable interannual fluctuations in post-monsoon water clarity. In 2020 and 2023, average NDTI values were negative, indicating clearer water conditions. Conversely, 2022 recorded the highest mean NDTI, suggesting a post-monsoon spike in turbidity, potentially due to sediment resuspension or anthropogenic disturbances following the monsoon. Interestingly, 2023 also shows the highest standard deviation among all years, highlighting significant spatial heterogeneity some areas may have been very clear, while others were significantly more turbid.

These findings underscore the complex and localized nature of sediment dynamics in the post-monsoon season, influenced by factors such as variable flow velocity, sediment deposition patterns, and human activities across different river zones.

Figure 4.16-Mean NDTI and Standard Deviation per Year (October)

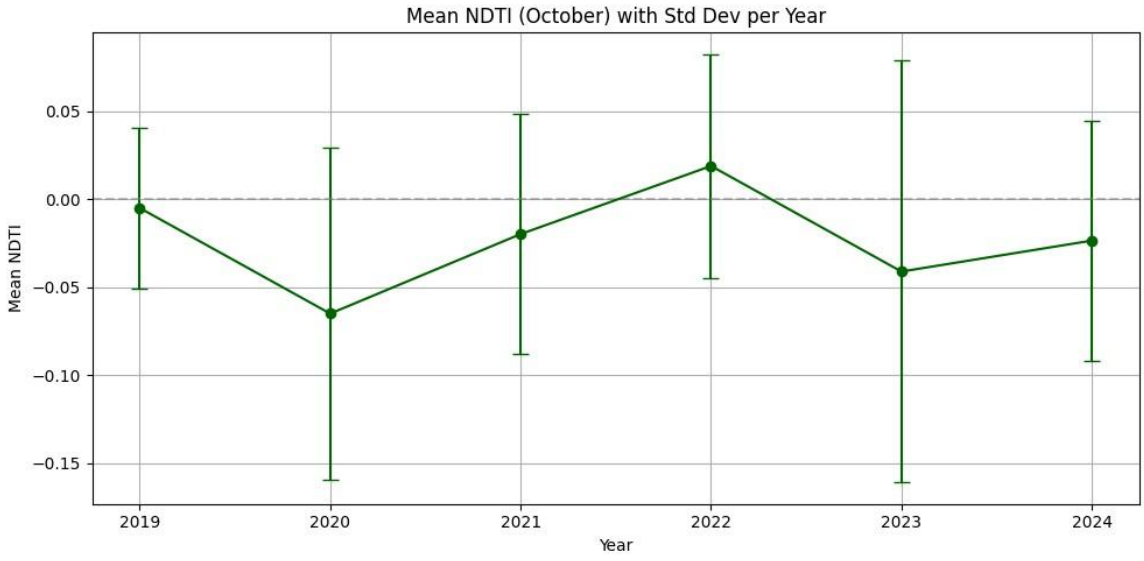

4.2.2 Standardized Temporal Analysis of Mean NDTI for October

Figure 4.17 illustrates the Z-score analysis of the mean Normalized Difference Turbidity Index (NDTI) for the month of October over the years 2019 to 2024. The Z-score standardization technique has been applied to normalize the inter-annual data, enabling a consistent comparison by expressing each year's deviation in terms of standard deviations from the overall mean.

A positive Z-score indicates that the turbidity in a particular year was above the long-term average, implying elevated levels of suspended particulate matter and potentially increased sediment input into the water body. In contrast, a negative Z-score reflects below-average turbidity, which may correspond to clearer water conditions during that period.

The analysis reveals a distinct anomaly in 2022, which recorded a Z-score of +1.57, signifying substantially higher turbidity compared to the multi-year mean. This peak suggests intensified sediment inflow or runoff, possibly linked to extreme monsoonal activity or anthropogenic disturbances. Meanwhile, the years 2020 and 2023 exhibit negative Z-scores, indicating lower turbidity levels, while the remaining years—2019, 2021, and 2024 hover close to the mean, representing relatively normal conditions.

The temporal variation observed in Z-scores highlights the dynamic nature of turbidity in the study area, which is likely influenced by seasonal hydrological processes, rainfall variability, and land-use changes within the catchment. Standardizing turbidity data through Z-scores provides a clearer understanding of inter-annual fluctuations and supports more robust interpretations of environmental changes affecting water quality.

Figure 4.17 – Z-Score Plot of Mean NDTI Values for October (2019–2024)

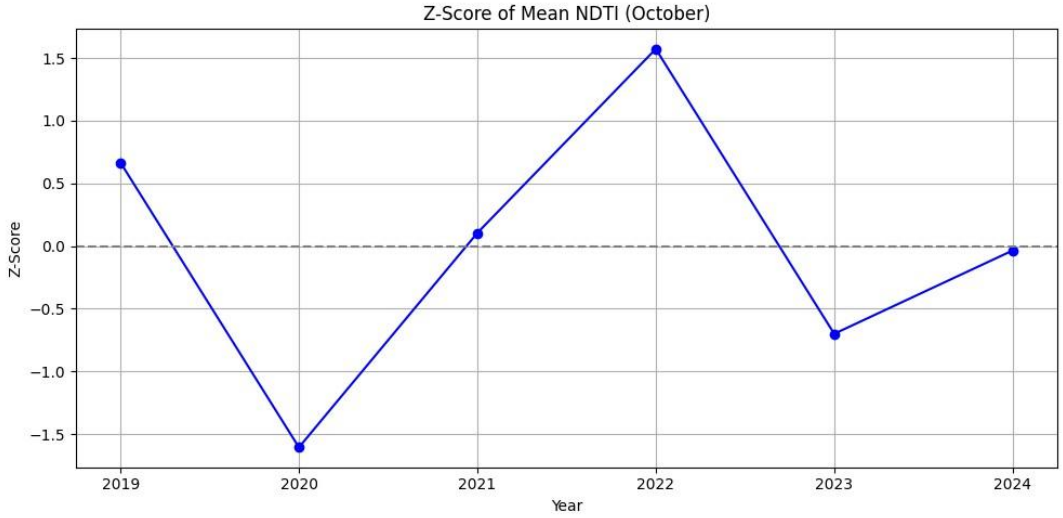

4.2.3 Linear Trend Analysis of Actual NDTI Values (October)

Figure 4.18 illustrates the temporal variation in mean Normalized Difference Turbidity Index (NDTI) values for the month of October from 2019 to 2024. The purple line with markers represents the actual recorded NDTI values for each year, capturing annual fluctuations in turbidity. The orange dashed line represents a linear regression fitted to these historical data points, summarizing the overall direction of change during the observed period. A grey horizontal line at NDTI = 0.00 is included as a neutral reference, where values above indicate more turbid conditions and values below suggest relatively clearer water.

The flat slope of the fitted regression line indicates that there is no consistent long-term increase or decrease in turbidity across the six-year span. This absence of a directional trend implies that October turbidity levels have remained relatively stable over time. The interannual variability seen in the actual NDTI values is more plausibly attributed to natural factors such as monsoonal runoff and seasonal hydrological dynamics, rather than sustained anthropogenic influences. This reinforces the interpretation that turbidity conditions in October are shaped predominantly by episodic environmental events rather than by long-term human activity.

Figure 4.18 – Linear Trend Analysis of Mean NDTI Values in October (2019–2024)

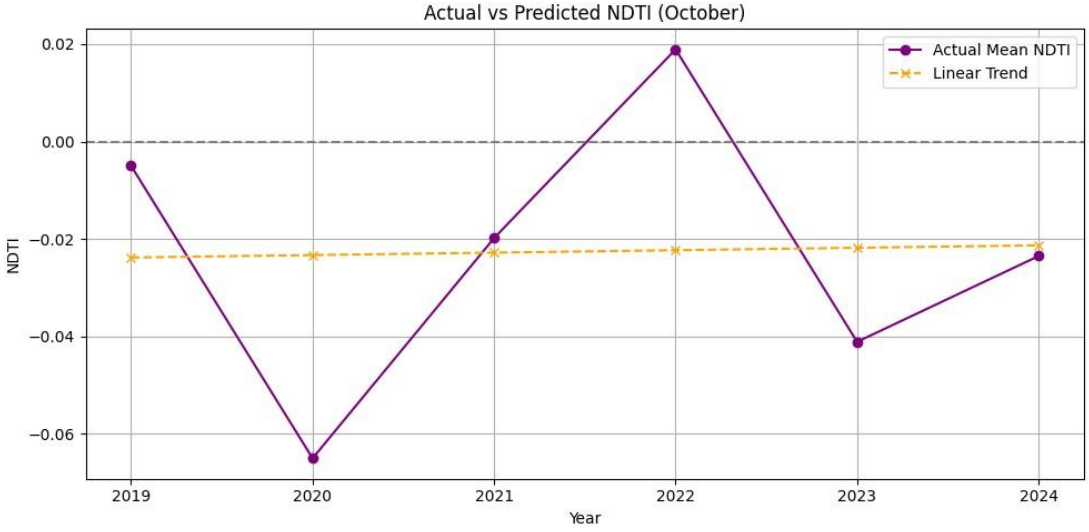

4.2.4 Spatial Distribution of Turbidity – NDTI Maps (October, 2019–2024)

Figures 4.19 to 4.24 display the spatial distribution of turbidity across the study area during October for the years 2019 to 2024, based on Normalized Difference Turbidity Index (NDTI) values. The colour gradient represents turbidity intensity, ranging from green (very low turbidity) to red (high turbidity). Green and yellow zones indicate clearer water with minimal sediment presence, while orange and red reflect increasing turbidity levels associated with greater suspended particulate matter.

Across the six-year period, most October maps are dominated by green and yellow zones, suggesting generally low turbidity levels. Orange zones, indicating moderate turbidity, appear more prominently in 2022 and 2024, particularly near Sangam and downstream areas, though red zones remain limited and highly localized. Compared to May, turbidity levels in October are notably lower, which aligns with the confirmed seasonal reduction in human activity, including religious gatherings and urban inflows, following the monsoon period.

These maps highlight spatial variability in turbidity that likely reflects the combined effects of hydrological changes, sediment transport, and reduced anthropogenic inputs. While no persistent hotspots are observed, the localized increases in 2022 and 2024 warrant closer monitoring to understand potential seasonal or episodic influences. The spatial patterns serve as a valuable supplement to temporal analyses by identifying specific areas where turbidity conditions vary from year to year.

Figure 4.19-NDTI Map 2019

Figure 4.20-NDTI Map 2020

Figure 4.21-NDTI Map 2021

Figure 4.22-NDTI Map 2022

Figure 4.23-NDTI Map 2023

Figure 4.24-NDTI Map 2024

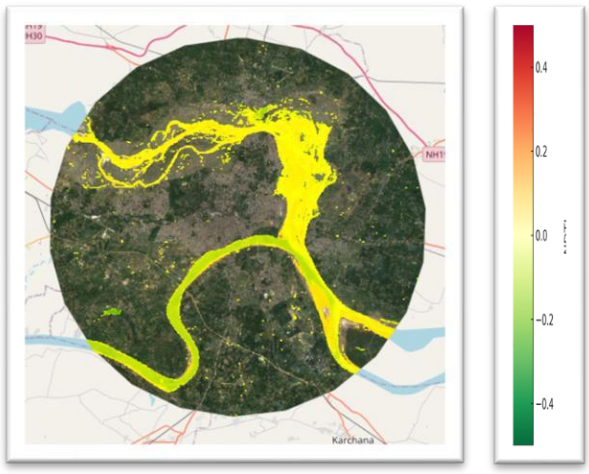

4.2.5 Inter-Annual Change in Turbidity – ΔNDTI Maps (October, 2019–2024)

Figures 4.25 to 4.29 present the ΔNDTI maps, which visualize the year-on-year changes in turbidity across the study area for October. These maps are derived by calculating the difference in Normalized Difference Turbidity Index (NDTI) values between consecutive years. Red regions indicate areas where turbidity increased relative to the previous year, while blue regions represent areas where water clarity improved. White zones denote minimal or no change in turbidity, suggesting relatively stable conditions.

The spatial patterns observed across the ΔNDTI maps show considerable variability from year to year. No consistent spatial trend is evident across the six-year period, and areas of increased or decreased turbidity shift geographically each year. For instance, while some sections of the river show higher turbidity in one year, those same areas may exhibit improved clarity in the following year. This indicates that turbidity dynamics in October are influenced by variable and localized factors rather than a linear or cumulative trend.

The absence of recurring spatial patterns and the alternating appearance of red and blue zones suggest that sediment load and water clarity in October are primarily driven by natural hydrological variability such as monsoonal runoff, catchment conditions, and flow changes rather than long-term pressure from regular surface activity. These ΔNDTI maps provide a useful diagnostic view for understanding short-term changes in river condition and highlight the spatially dynamic nature of turbidity during the post-monsoon season.

Figure 4.25-ΔNDTI (2020–2019)

Figure 4.26-ΔNDTI (2021–2020)

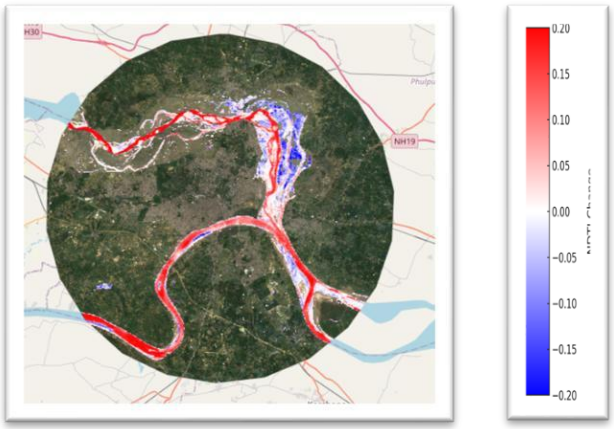

Figure 4.27-ΔNDTI (2022–2021)

Figure 4.28-ΔNDTI (2023–2022)

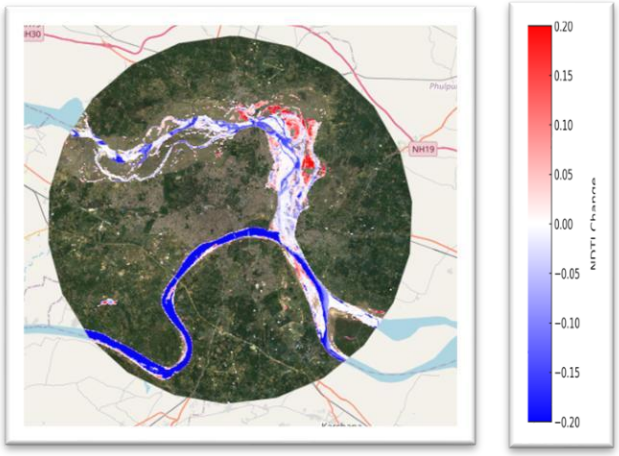

Figure 4.29-ΔNDTI (2024–2023)

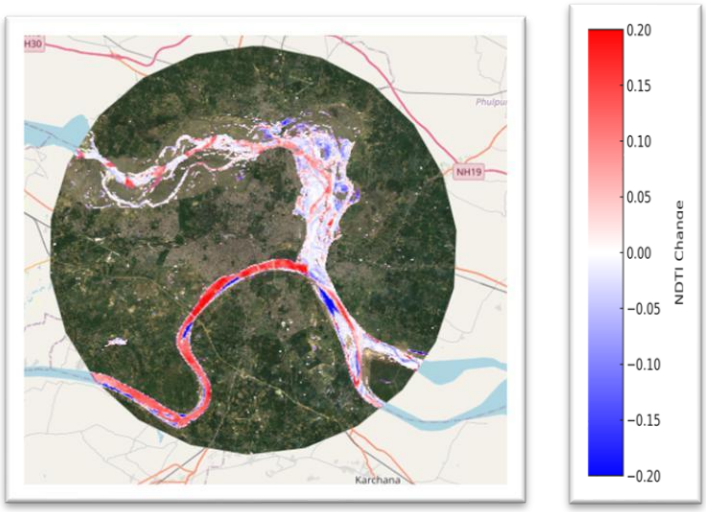

4.2.6 Year-on-Year Change in NDTI (Compound ΔNDTI) with Standard Deviation

Figure 4.30 presents the compound year-on-year changes in the Normalized Difference Turbidity Index (ΔNDTI) for the month of October, accompanied by standard deviation bars to reflect spatial variability. Each bar represents the average change in turbidity across the study area compared to the previous year, while the standard deviation indicates the degree of heterogeneity in turbidity change across different locations.

The data show that turbidity increased in 2021, 2022, and 2024, as indicated by positive ΔNDTI values, with the highest increase observed in 2021–2020 (ΔNDTI ≈ +0.045). In contrast, 2020 and 2023 recorded negative ΔNDTI values, suggesting an overall reduction in turbidity across the river stretch. The most significant decreases occurred during 2020–2019 and 2023–2022, both with ΔNDTI values around –0.06. Standard deviation values range from moderate to relatively high, with some years exhibiting spatial variability as large as ±0.10 to ±0.12. This indicates that while overall trends in turbidity may appear increasing or decreasing at the basin level, local conditions can diverge significantly, reinforcing the need for fine-scale analysis alongside aggregated metrics.

The compound ΔNDTI analysis, when interpreted together with spatial maps, supports the conclusion that turbidity dynamics during October are governed by both annual hydrological variations and site-specific sediment processes, rather than uniform trends across the entire river system.

Figure 4.30 – Inter-Annual Change in Compound ΔNDTI with Standard Deviation (October, 2019–2024)

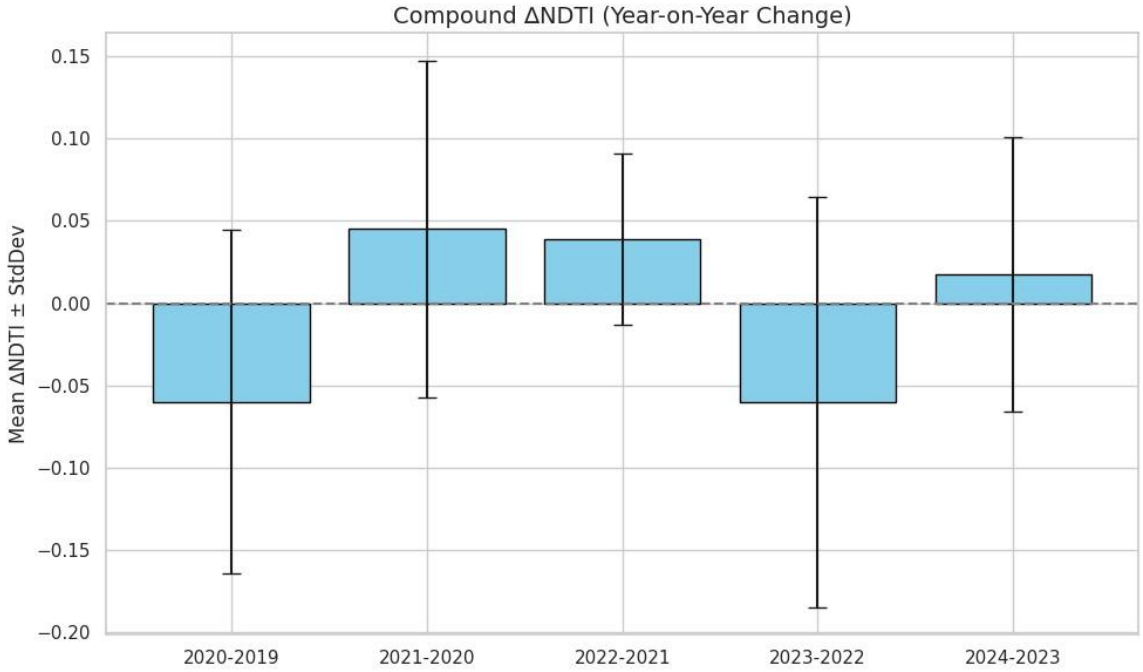

4.3 Seasonal Comparison

4.3.1 Seasonal Comparison of Mean NDTI (May vs October)

Figure 4.31 illustrates the comparative analysis of average NDTI values recorded in the months of May and October from 2019 to 2024. The blue line represents May (pre-monsoon), and the orange line represents October (post-monsoon).

The pattern shows that May generally exhibits higher turbidity levels in most years especially in 2020, 2023, and 2024 indicating a greater presence of suspended sediments. This can be attributed to increased anthropogenic activity such as ritual bathing, tourism, and lower river discharge during the summer season. However, exceptions are observed in 2019, 2021, and 2022, where October values are higher, likely influenced by post-monsoon runoff and sediment redistribution.

These fluctuations suggest that while May is typically marked by human-induced turbidity, October turbidity is more variable and driven by natural hydrological processes. The seasonal contrast highlights the importance of analysing both anthropogenic and environmental drivers in evaluating river water clarity over time.

Figure 4.31 – Yearly Average Turbidity Comparison for May (Blue) and October (Orange), 2019–2024

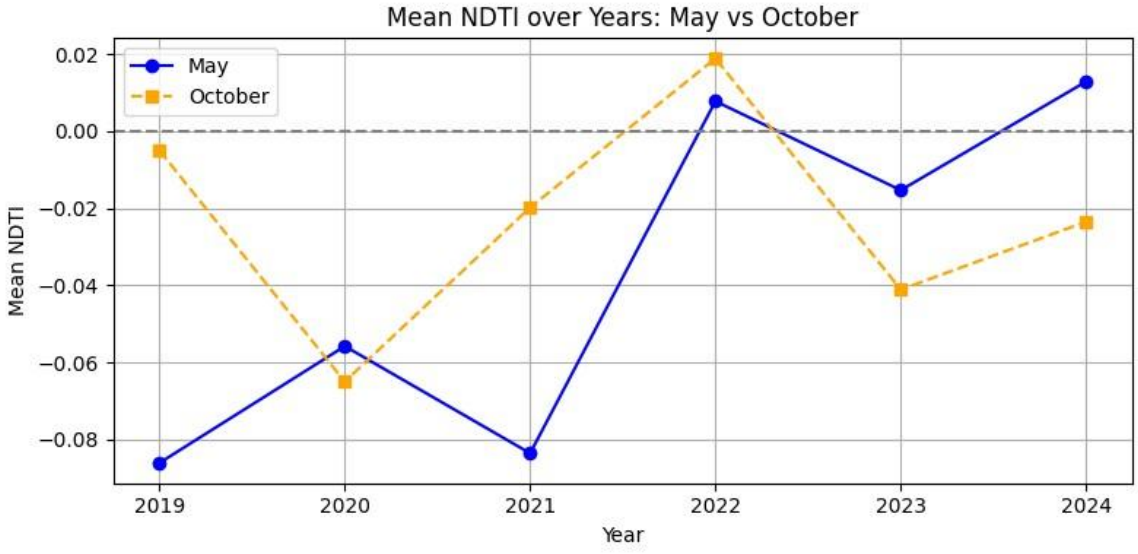

4.3.2 Mean NDTI with Standard Deviation (May vs October), 2019–2024

Figure4.32 illustrates inter-annual changes in turbidity for May and October, accompanied by standard deviation error bars to indicate spatial variability. Across all six years, May exhibits lower standard deviations compared to October, confirming that turbidity during this month is more spatially consistent. This pattern aligns with the fact that May consistently shows lower error bars, indicating minimal variation across the river surface. Conversely, October displays noticeably higher standard deviations in all years, especially from 2022 to 2024, reflecting greater spatial heterogeneity in turbidity conditions. This variability suggests that turbidity in October is unevenly distributed across the river channel. Additionally, October values show wider fluctuations in mean NDTI, including both the highest (2022) and lowest (2020) mean values in the dataset. In contrast, May shows a steady upward trend in mean NDTI from 2021 to 2024 with comparatively stable variability. These findings confirm that October turbidity exhibits more irregular spatial and temporal patterns, while May turbidity remains more uniform and progressively increasing over time

Figure 4.32-mean values with error bars (spatial variability).

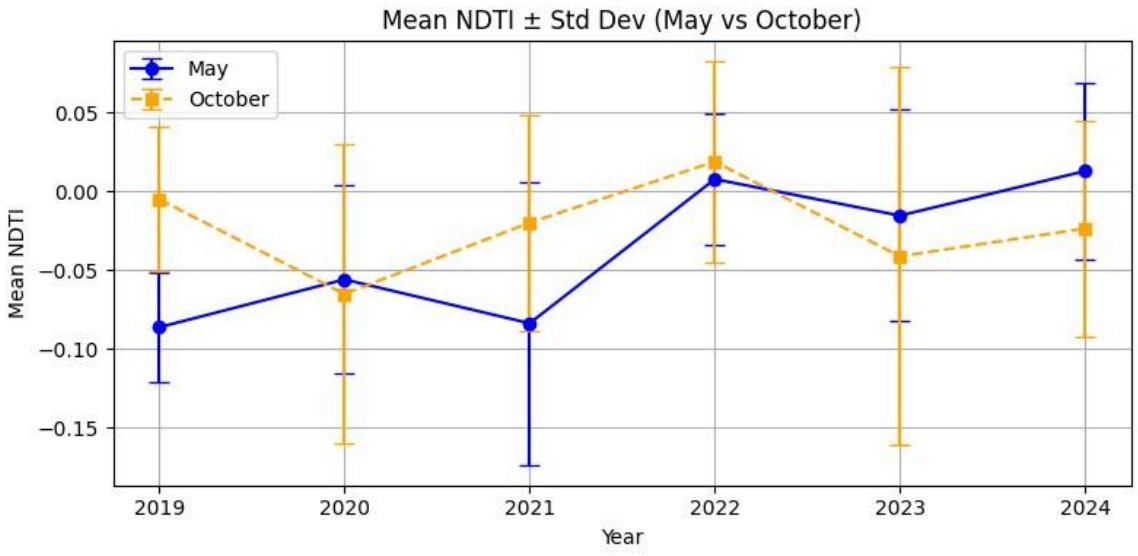

.

Figure 4.3.3 Bar Graph: Standard Deviation of NDTI (May vs October, 2019–2024)

This bar graph highlights the yearly spatial variability in turbidity for May and October using the standard deviation of NDTI values. Across most years, October shows consistently higher standard deviation than May, indicating more spatially uneven turbidity distribution. The peak variability occurs in October 2023 (~0.12), suggesting localized disturbances or runoff effects. In contrast, May displays lower and more stable variability, with values generally between 0.04 and 0.09, reflecting more uniform sediment spread likely due to crowd-driven activity across common zones. The observed pattern reinforces that October turbidity is more location-dependent, while May reflects consistent anthropogenic influence across the river stretch.

Figure 4.33-Bar graph comparing yearly spatial variability in turbidity

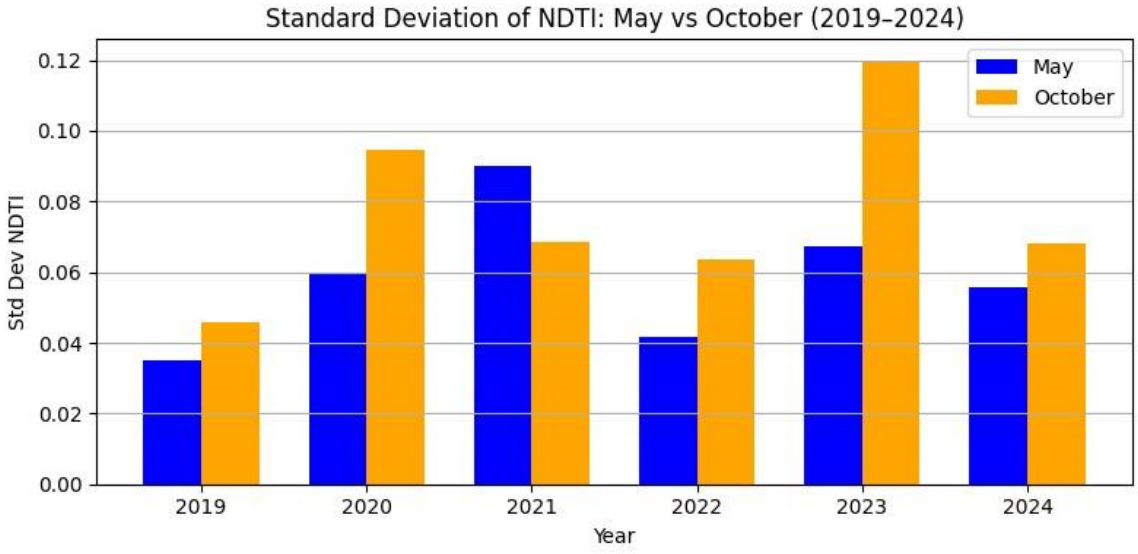

4.3.4 Z-Score of Mean NDTI: May vs October (2019–2024)

This bar graph presents standardized NDTI values (Z-scores) to assess how each year's turbidity deviated from the long-term mean. A Z-score of 0 indicates average turbidity for the study period, while positive and negative values reflect above- and below-average turbidity, respectively.

From the graph, May shows a transition from negative to consistently positive Z-scores post-2022, indicating a steady rise in turbidity levels relative to the long-term average likely linked to sustained anthropogenic activity.

In contrast, October displays a more irregular pattern, with both high and low deviations across years, reflecting the influence of variable natural factors such as post-monsoon runoff, sediment resettlement, or changing flow conditions. The higher volatility in October scores underlines the less predictable, environmentally-driven nature of turbidity in that season

Figure 4.34-Standardized NDTI values (Z-scores) for May and October each year.

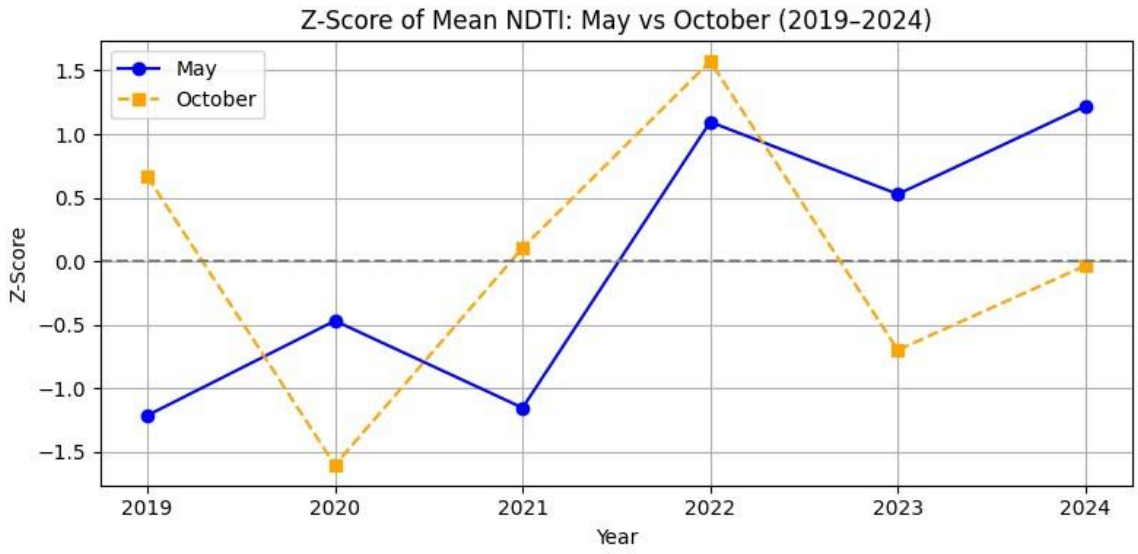

4.3.5 Linear Trend in NDTI (May vs October, 2019–2024)

Figure 4.35 presents a linear trend analysis of the observed NDTI values for May and October from 2019 to 2024. While not predictive, the linear fit offers a visual summary of the direction of turbidity change across the years. The trend for May shows a gradual increase in NDTI values, suggesting a steady rise in turbidity that may be attributed to consistent anthropogenic pressures during the pre-monsoon period. In contrast, the trend for October appears relatively flat, indicating no clear directional change over time. This suggests that turbidity in October is governed more by natural post-monsoon processes such as sediment inflow and runoff variability rather than recurring human activity. The comparison underscores that May turbidity reflects a progressive pattern, whereas October turbidity remains more spatially and temporally variable.

Figure 4.35-Linear trend line for both May and October NDTI values.

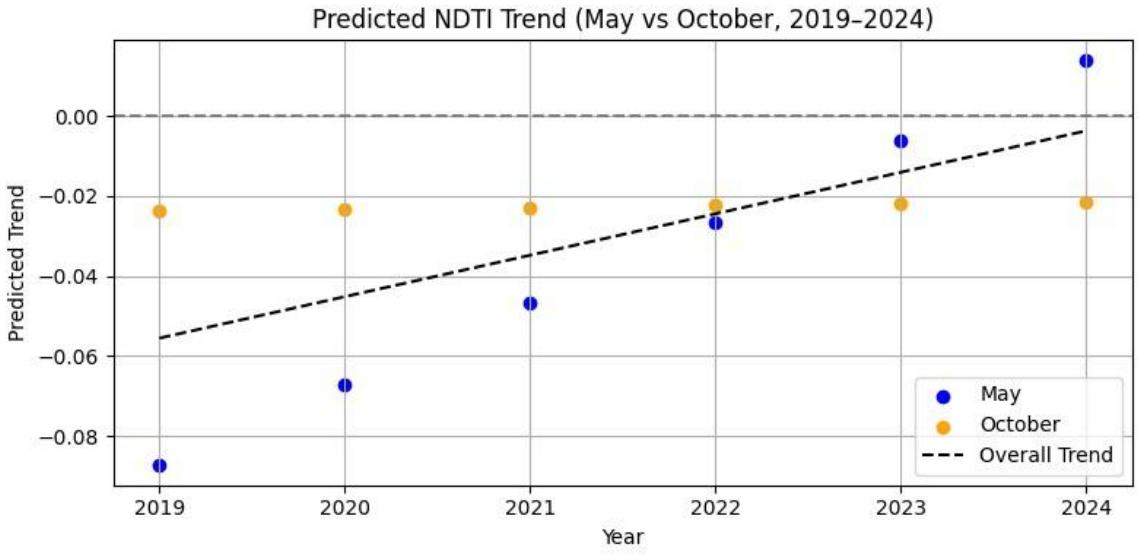

5. CONCLUSION

This study revealed distinct seasonal and spatial patterns in river turbidity across the Prayagraj region between 2019 and 2024 using the Normalized Difference Turbidity Index (NDTI). During the pre-monsoon season (May), turbidity was consistently higher near active ghats, where mass gatherings and direct river entry occurred. In contrast, the post monsoon season (October) showed turbidity patterns driven mainly by natural factors, such as monsoon runoff, bank erosion, and sediment resettlement, with only limited human influence.

The use of compound ΔNDTI analysis allowed detection of year-on-year turbidity fluctuations, which alternated between increases and decreases highlighting the river system's sensitivity to both anthropogenic and hydrological changes. Spatial ΔNDTI maps further pinpointed localized zones of disturbance, especially near populated ghats.

Overall, the findings confirm that human-induced turbidity is dominant during dry months, while natural processes control sediment dynamics after the monsoon, emphasizing the importance of season-specific monitoring and intervention strategies.

6. REFERENCES

6.1 Academic Literature

Alparslan, E., Aydöner, C., Tufekci, V., & Tüfekci, N. (2007). *Water quality assessment at Ömerli Dam using remote sensing techniques.* Environmental Monitoring and Assessment, 135(1), 391–398.
Referenced for traditional vs remote turbidity monitoring.

Nechad, B., Ruddick, K., & Neukermans, G. (2010). *Calibration and validation of a generic multisensor algorithm for mapping turbidity in coastal waters.* Remote Sensing of Environment, 114(4), 854–866.
Cited for NDTI formulation and limitations.

Kundu, S., Nath, D., & Kar, S. (2021). *Assessing sediment transport in the Ganga River using remote sensing-based turbidity indices.*
Referenced in support of NDTI use in Indian rivers.

Chawla, I., Singh, O., & Jain, S. K. (2022). *Monitoring seasonal water quality variation using satellite-derived indices in large river basins.* Supports regional seasonal turbidity analysis.

Singh, R., Kumar, A., & Shukla, R. (2015). *Impact of Kumbh Mela on water quality of Ganga River at Allahabad.* Indian Journal of Environmental Protection, 35(5), 402–408.

Used to link Mela events with observed turbidity peaks.

Martínez, L., et al. (2021). *River sediment shift detection using year-on-year change indices.*
Cited for ΔNDTI spatial change interpretation.

6.2 Statistical & Geospatial Tools

Google Earth Engine. (n.d.). *Google Earth Engine Data Catalog.*
Retrieved from: https://developers.google.com/earth-engine/datasets For Sentinel-2 access, .reduceRegion(), .map() use.

Copernicus Open Access Hub. (2015). *Sentinel-2 MSI: Multispectral Instrument, Level2A.*
Retrieved from: https://scihub.copernicus.eu/ Source of Sentinel-2 SR imagery.

Folium Documentation. (n.d.).

https://python-visualization.github.io/folium/ Used
for interactive ghat mapping.

Geemap Documentation. (n.d.).
https://geemap.org/
Used to integrate Earth Engine with Python for analysis and plotting.

Scikit-learn (sklearn). (n.d.).
https://scikit-learn.org/
Used for linear regression modeling.

6.3 Government & Institutional Reports

Central Pollution Control Board (CPCB). (2019). *Report on Water Quality During Kumbh Mela.*
Used in sections evaluating ghat influence on turbidity.

Prayagraj Mela Authority. (2023). *Official Mela Crowd Management Report.*
Used for validating crowd presence near ghats in May and October.